Double-layered perovskite positive electrode with high capacity involving O–O bond formation for all-solid-state fluoride-ion batteries

Lithium-ion batteries (LIBs) are widely used in various electronic devices owing to their high energy density, high power density, and long-term durability. However, with the growing demand for longer-range electric vehicles, there is a need to develop high-energy-density batteries that do not rely on lithium. One strategy to surpass the energy density of current LIBs is to utilize electrode materials that enable multielectron reactions. However, using polyvalent ions such as magnesium ions (Mg^{2+}) as carriers presents kinetic disadvantages, such as slow diffusion within solid electrodes. In contrast, fluoride ions (F^-), which are monovalent and have a small ionic radius (1.33 Å), can enable multielectron reactions with fast ionic conduction. Owing to these characteristics, all-solid-state fluoride-ion batteries (FIBs) that use F^- as a carrier have attracted attention for their potential to achieve high energy and power densities [1,2]. While metal/metal fluorides have been developed as typical positive electrodes, they suffer from poor cyclability and power density due to large volume changes during charging and discharging. To address these issues, electrode materials based on topotactic F^- intercalation reactions have been developed. Compared to metal/metal fluorides, these materials significantly improve cyclability and power density. However, their usable capacity is limited because of their relatively large chemical formula weight. In this study, to increase the capacity of intercalation-type positive electrode materials, anion redox, as reported in LIB cathodes [3], was applied to a double-layered perovskite $La_{1.2}Sr_{1.8}Mn_2O_{7-\delta}F_2$ [4].

The $La_{1.2}Sr_{1.8}Mn_2O_{7-\delta}F_2$ delivered a charge capacity of approximately 250 mA·h/g (Fig. 1(a)) after the initial discharge. The subsequent discharge yielded a large capacity of 190 mA·h/g, nearly double the initial discharge. Excess electrochemical fluorination was confirmed to be topotactic through X-ray diffraction (XRD), scanning transmission electron microscopy (STEM) and atomic resolution electron energy loss spectroscopy (EELS). The XRD pattern of the 3.0 V charged $La_{1.2}Sr_{1.8}Mn_2O_{7-\delta}F_2$ remained similar to that of the pristine state (Fig. 1(b)), while STEM imaging indicated regular cation arrangements (Fig. 1(c)). EELS mapping of the 3.0 V charged $La_{1.2}Sr_{1.8}Mn_2O_{7-\delta}F_2$ (Fig. 1(c)) revealed the presence of excess F^- in the perovskite block alongside the interstitial site within the rock-salt slabs. Upon discharge, the defluorinated

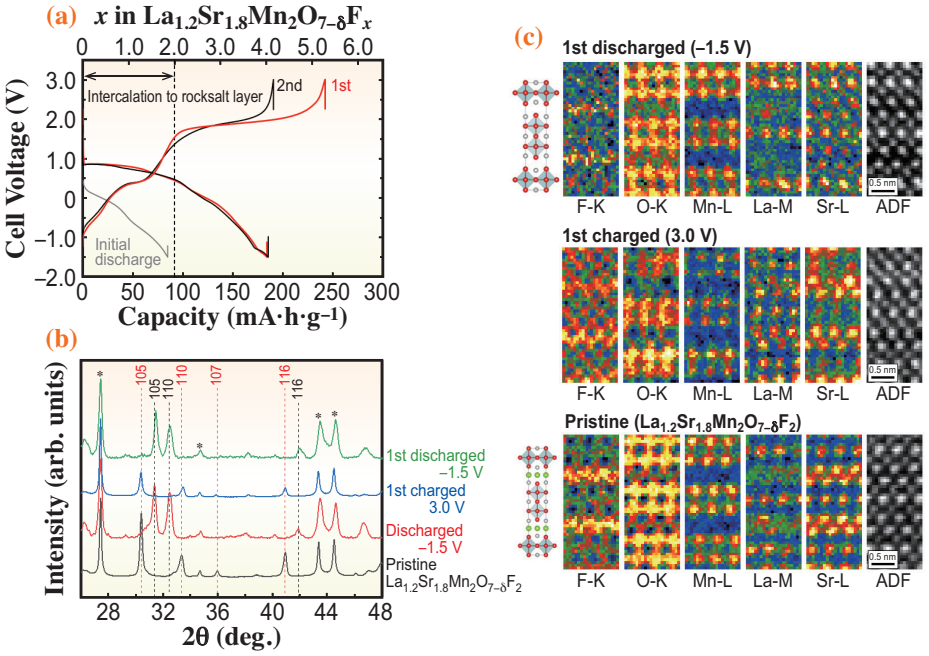

Fig. 1. **(a)** Charge/discharge curves of $La_{1.2}Sr_{1.8}Mn_2O_{7-\delta}F_2$. **(b)** XRD patterns of cathode composites containing $La_{1.2}Sr_{1.8}Mn_2O_{7-\delta}F_2$ during charge/discharge. Red and black broken lines correspond to $La_{1.2}Sr_{1.8}Mn_2O_{7-\delta}F_2$ and $La_{1.2}Sr_{1.8}Mn_2O_{7-\delta}$, respectively. Asterisks denote the $La_{0.9}Ba_{0.1}F_{2.9}$ electrolyte. **(c)** Atomic resolution STEM-EELS mapping images of $La_{1.2}Sr_{1.8}Mn_2O_{7-\delta}F_2$ during charge/discharge along the [010] crystallographic axis.

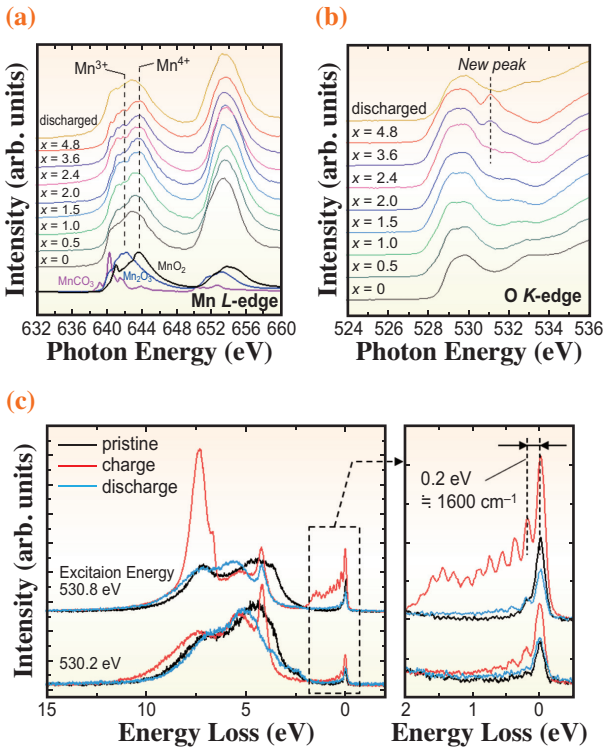

Fig. 2. **(a)** Mn *L*-edge and **(b)** O *K*-edge XAS spectra collected at SPring-8 **BL27SU** of $La_{1.2}Sr_{1.8}Mn_2O_{7-\delta}F_2$ during charge/discharge. The parameter x in the figure represents the fluoride content (x in $La_{1.2}Sr_{1.8}Mn_2O_{7-\delta}F_x$). **(c)** O *K*-edge RIXS spectra recorded at excitation energies of 530.2 and 530.8 eV at SPring-8 **BL07LSU** for the pristine, charged (3.0 V), and discharged (–1.5 V) states, respectively.

$La_{1.2}Sr_{1.8}Mn_2O_{7-\delta}$, phase was identified by both XRD and EELS (Figs. 1(b,c)). The charge compensation mechanism during (de)fluorination was analyzed using soft X-ray absorption spectroscopy (XAS) and resonant inelastic X-ray scattering (RIXS) (Fig. 2). The Mn *L*-edge spectrum of $La_{1.2}Sr_{1.8}Mn_2O_{7-\delta}F_2$ (Fig. 2(a)) showed a shift to higher energy from $x = 0$ to $x = 2.0$ but no further shift was observed from $x = 2.0$ to $x = 4.8$. This behavior indicates that Mn ions are oxidized from Mn^{3+} to Mn^{4+} during the initial charging phase and remain as Mn^{4+} in the later stage of charge. In the O *K*-edge spectrum, the intensity at 529 eV increased during the early stage of charging ($x < 2$) (Fig. 2(b)) owing to the oxidation of Mn^{3+} to Mn^{4+}. However, as charging progressed beyond $x \sim 2$, a new O *K*-edge peak emerged at ~530.8 eV. The intensity of this peak increased with further charging and reversibly disappeared upon discharge. To investigate the origin of this new peak, RIXS measurements were performed at excitation energies between 528.5 and 533.0 eV. The RIXS spectra at 530.8 eV (Fig. 2(c)) revealed discrete energy loss peaks near the elastic line from 5 to 0 eV. The vibrational frequency of the first level was measured at 1591 cm^{-1}, closely matching the molecular O_2 (~1600 cm^{-1}), observed in charged $Na_{0.75}[Li_{0.25}Mn_{0.75}]O_2$ by RIXS [5]. This result indicates the formation of an O–O bond in charged $La_{1.2}Sr_{1.8}Mn_2O_{7-\delta}F_2$. Upon discharge, this vibration signature disappeared, confirming the reversible nature of O–O bond formation/breaking.

These results demonstrate that $La_{1.2}Sr_{1.8}Mn_2O_{7-\delta}F_2$ undergoes two distinct fluoride (F^-) intercalation processes: initial (de)intercalation into rock-salt slabs with conventional Mn redox and subsequent (de)intercalation of excess F^- into the perovskite layer involving the formation of an oxygen–oxygen bond (anion redox) (Fig. 3). This study is the first to demonstrate the introduction of electronic holes and the associated formation of O–O bonds following the electrochemical intercalation of an anionic species. Given the abundance of perovskite compounds, these findings are expected to advance the development of cathode materials for FIBs, where mixed-anion compounds with anion redox reactions may serve as effective active materials.

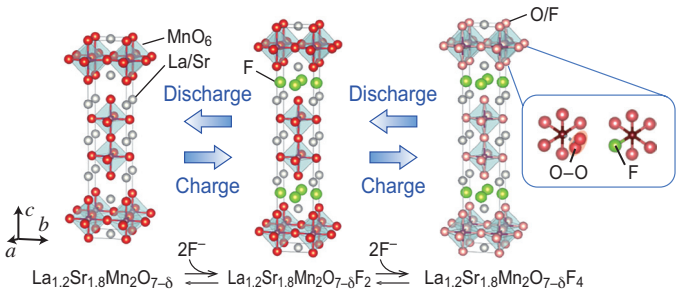

Fig. 3. Discharge/charge scheme of $La_{1.2}Sr_{1.8}Mn_2O_{7-\delta}F_2$. The specific locations of the O–O bond and excess F^- in the charged $La_{1.2}Sr_{1.8}Mn_2O_{7-\delta}F_2$ are not clear.

Kentaro Yamamoto

Faculty of Engineering, Nara Women's University

Email: k.yamamoto@cc.nara-wu.ac.jp

References

[1] M. Anji Reddy and M. Fichtner: J. Mater. Chem. **21** (2011) 17059.
[2] D. Zhang *et al.*: ACS Appl. Mater. Interfaces **13** (2021) 30198.
[3] M. Sathiya *et al.*: Nat. Mater. **12** (2013) 827.
[4] *H. Miki, K. Yamamoto, H. Nakaki, T. Yoshinari, K. Nakanishi, S. Nakanishi, H. Iba, J. Miyawaki, Y. Harada, A. Kuwabara, Y. Wang, T. Watanabe, T. Matsunaga, K. Maeda, H. Kageyama, Y. Uchimoto: J. Am. Chem. Soc.* ***146*** *(2024) 3844.*
[5] R. A. House *et al.*: Nature **577** (2020) 502.